Journal of Crystal Growth 318 (2011) 500–504

Contents lists available at ScienceDirect

Journal of Crystal Growth

journal homepage: www.elsevier.com/locate/jcrysgro

Optical properties of (1 $\bar{1}$ 0 1) semi-polar InGaN/GaN multiple quantum wells grown on patterned silicon substrates

Ching-Hsueh Chiu [a], Da-Wei Lin [a], Chien-Chung Lin [c], Zhen-Yu Li [a], Yi-Chen Chen [a], Shih-Chun Ling [a,b], Hao-Chung Kuo [a,*], Tien-Chang Lu [a], Shing-Chung Wang [a], Wei-Tsai Liao [b], Tomoyuki Tanikawa [d], Yoshio Honda [d], Masahito Yamaguchi [d], Nobuhiko Sawaki [e]

[a] Department of Photonics & Institute of Electro-Optical Engineering, National Chiao Tung University, 1001 Ta Hsueh Road, Hsinchu 30010, Taiwan
[b] Department of Opto-Electronics Epitaxy and Devices, Industrial Technology Research Institute, Rm. 206, Bldg 78, 195, Section 4, Chung Hsing Rd., Chutung, Hsinchu 31040, Taiwan
[c] Institute of Photonic System, College of Photonics, National Chiao-Tung University, No.301, Gaofa 3rd. Road, Guiren Township, Tainan County 71150, Taiwan
[d] Department of Electronics, Nagoya University, 3C-1, Furo-cho, Chikusa, Nagoya, Aichi, 464-8603, Japan
[e] Department of Electrical & Electronic Engineering, Aichi Institute of Technology, 1247 Yachigusa, Yakusa, Toyota 470-0392, Japan

ARTICLE INFO

Available online 23 October 2010

Keywords:
A3. Metalorganic chemical vapor deposition
A3. Quantum wells
B1. Nitride
B2. Semiconductor III–V materials
B3. Light emitting diode

ABSTRACT

We present a study of high quality (1 $\bar{1}$ 0 1) GaN films and the InGaN/GaN multiple quantum wells (MQWs) using epitaxial lateral overgrowth (ELO) technique by atmospheric pressure metal organic chemical vapor deposition (MOCVD). The smooth coalescence of the stripes and surface morphology was measured by scanning electron microscope (SEM) and atomic force microscopy (AFM). Due to reduction in internal electric field, semipolar InGaN/GaN MQWs have higher radiative recombination rate from time-resolved photoluminescence (TRPL) measurement. In addition, from degree of polarization (DOP) measurement, we observed higher polarization ratio attributed to the induced anisotropic compressive strain.

1. Introduction

GaN semiconductor has been widely used for electronic and optical devices [1–3]. However, the conventional c-plane quantum wells suffer the quantum-confined Stark effect (QCSE) as a result of the existence of spontaneous and piezoelectric polarization fields parallel to [0 0 0 1] c direction [4]. This effect restricts the carrier recombination efficiency, reduces oscillator strength, and induces red-shift photon emission. So it is natural to expect that the quantum wells grown on semipolar GaN, such as {1 $\bar{1}$ 0 1} GaN [5] and {1 1 $\bar{2}$ 2} GaN [6], can exhibit lower QCSE, and the luminescence efficiency and wavelength stability are expected to be better [7,8].

Because of the difficulties to growth pure GaN substrates, most of GaN-based epitaxial wafers were grown on sapphire, or SiC, or pure silicon wafers. Although sapphire touts low cost of production and it is the most widely used substrate material, the low thermal and electrical conductivities make it less perfect as a substrate for the GaN epilayers. While the high price and some mechanical defects hinder SiC substrate's acceptability in the LED market, silicon has been considered as an alternative substrate due to its low manufacturing cost, large size, and good thermal and electrical conductivities [9].

However, there are still several problems using Si substrate for GaN the epilayer. The lattice mismatch between GaN and Si is almost 17% which lead to high threading dislocation densities (TDDs) (around 10^9–10^{11} cm^{-2}) in the GaN epilayer. Another major problem is that the thermal expansion coefficient difference between two materials is as large as 56%, which induces a high tensile stress during the cooling process and often results in cracks and damages of epilayers [10]. Without resolving these two problems, GaN growth on Si is not practical enough for commercial success. One approach to mitigate these problems is to use patterned silicon wafers for selective area growth (SAG) and ELO. To obtain SAG of GaN, Mao et al. [11] and Marchand et al. [12] have used predeposited GaN/AlN on (1 1 1) Si and predeposited AlN on (1 1 1) Si as substrates, respectively. Also, Kobayashi et al. [13] have demonstrated SAG of GaN using AlO_x /(1 1 1)Si substrates. Following a similar thought, Nagoya University also demonstrated that by using SiO_2 nano mask and SAG, great quality of semipolar GaN film can be grown on Si substrate [14–16], and great progress has been presented in terms of the reduced density of the threading dislocation in GaN grown on Si substrate. Nevertheless, the optical properties of semipolar InGaN/GaN multiple-quantum wells (MQWs) grown on (1 $\bar{1}$ 0 1) GaN/ tilt degrees off axis (0 0 1) Si substrate have not been reported yet. In this work, we investigate the growth evolution of GaN on tilt degrees off axis (0 0 1) Si substrate. Moreover, the dynamic optical property of the

* Corresponding author.
E-mail addresses: chienchunglin@faculty.nctu.edu.tw (S.-C. Ling), hckuo@faculty.nctu.edu.tw (H.-C. Kuo).

0022-0248/$ - see front matter © 2010 Published by Elsevier B.V.
doi:10.1016/j.jcrysgro.2010.10.054

semipolar (1 $\bar{1}$ 0 1) InGaN/GaN MQW grown on the (1 $\bar{1}$ 0 1) GaN templates are investigated and compared to those of the polar (0 0 0 1) InGaN/GaN MQW grown on (0 0 0 1) GaN/(1 1 1) Si. From the experimental results, we can demonstrate that superior quality of semi-polar InGaN/GaN film was achieved by this specialized patterned silicon substrates.

2. Experiment procedure

The schematic growth process is shows in Fig. 1 (a)–(c). First, we prepared a (0 0 1) silicon substrate, whose $<0\,0\,1>$ axis tilts 7 degrees toward the $<1\,1\,0>$ direction, followed by the deposition of 70-nm-thick SiO_2 film as the etching mask. Then, stripe masks parallel to the $<\bar{1}\,1\,0>$ of the Si substrate with a period of 2 μm (window)/1 μm (stripe) were made by conventional photolithography. Subsequently, the samples were immersed into 30% KOH solution at 60 °C for 2 min to obtain 1-μm-depth patterned grooves. The ($\bar{1}\,\bar{1}$ 1) facet of the groove sidewalls was passivated by SiO_2 deposition and (1 1 1) facet was exposed to air for the GaN growth as shown in Fig. 1(a). Thereafter, the patterned Si substrate was loaded into atmospheric pressure metal organic chemical vapor deposition (MOCVD) chamber for epitaxial growth. The GaN was grown selectively on a (1 1 1) facet via an AlN buffer layer. As the heat treatment prior to the deposition of the AlN buffer layer, TMA (5.52 μmol/min) was supplied for 30 s at 1000 °C. Then an AlN buffer layer was deposited at 1150 °C by supplying (TMA:NH_3)=(5.52 μmol/min:2.5 slm) for 4 min, and the estimated thickness is 100 nm. After the formation of the AlN buffer layer, the SAG of GaN was deposited at 1100 °C for 50 min by supplying (TMG:NH_3)=(18.3 μmol/min:2.5 slm). At high growth temperature, micro-meter size GaN pyramidal structure was formed on the (1 1 1) Si surface as shown in Fig. 1(b). When more materials were added on the seed layer, GaN between the adjacent patterned stripes would coalesce and finally a uniform (1 $\bar{1}$ 0 1) GaN film is show in Fig. 1(c).

Next, we deposited the InGaN/GaN MQWs structure on this semi-polar GaN template by MOCVD. During the growth, trimethylgallium (TMGa), trimethylindium (TMIn) and ammonia (NH_3) were used as gallium, indium, and nitrogen sources, respectively. Hydrogen (H_2) and nitrogen (N_2) were used as the carrier gases. In the full LED epitaxial layer structure, we have 6 pairs of InGaN/GaN quantum wells on the semi-polar GaN template. Two different growth temperatures (1100 °C, and 1030 °C) were used to find out their correlation to crystal quality. On the other hand, the same InGaN/GaN active layer structure was also grown on planar (1 1 1) Si substrate for comparison, denoted as conventional LEDs.

In the subsequent experiments, we used AFM, CL, and various PL technologies to examine our grown InGaN/GaN film. The AFM was performed right after seed GaN layer finished its coalesce such that we could check the surface morphology of epitaxial layer. The spatially resolved CL imaging was obtained by scanning electron microscope (JEOL-7000F SEM system) with a fixed viewing scale. The temperature dependent PL measurements were done by a 325 nm He-Cd laser at 25 mW excitation power and the emitted luminescence light was collected through a 0.32 m spectrometer with a charge-coupled device detector. The focused spot size of the laser was estimated to be about 200 μm in diameter. Low temperature TRPL measurements were performed at 10 K using the 385 nm line of a tunable Ti: sapphire laser, which provides a laser pulse width of 200 fs and the repetition rate is 76 MHz, as the excitation source. The luminescence spectrum was measured by a 0.55 m monochromator and detected by a microchannel plate photomultiplier tube (MCP-PMT tube). The temporal resolution is 88 ps in our measurement.

3. Results and discussion

The growth of the nano-facet is similar to self-organized one on substrates with periodic patterns designed for quantum dot growth [17] in which the two-dimensional growth of preferred crystalline orientation can be achieved by strain-balance in the layer. In current situation, a smooth (1 $\bar{1}$ 0 1) GaN face could be formed when substrate's Si $<0\,0\,1>$ axis tilts 7 degrees toward the Si $<1\,1\,0>$ direction. This tilt angles off axis (0 0 1) Si substrate is very important. Fig. 2 show cross-section SEM image of the GaN film on patterned Si substrate. The appearance of the step like structure was mainly determined by the other degrees off axis angle as well as the direction of the stripe mask on the Si substrate is shown in Fig. 2(a). We can obtain a smooth (1 $\bar{1}$ 0 1) GaN surface when the substrate is 7 degrees off axis (0 0 1) Si as shown in Fig. 2(b). By this procedure, we achieved a platelet of (1 $\bar{1}$ 0 1) GaN based on the coalesced GaN stripes is shown inset of Fig. 2(b).

The quality of the film can be evaluated by its surface roughness. After the undoped GaN (u-GaN) layer was deposited, the surface morphology was measured by atomic force microscopy (AFM), as shown in Fig. 3(a) and (b). The root mean square (RMS) value of the surface roughness is about 5.9 nm and 0.7 nm on the 6.5 degrees off axis and 7 degrees off axis angle, respectively. It indicates high surface quality and excellent coalescence of the stripes is very orientation-sensitive

In addition to surface morphology, the quality of InGaN quantum wells on this semi-polar GaN surface is of the same importance. We tried two different growth temperatures as mentioned before (1100 °C and 1030 °C). Cathodoluminescence was applied to judge epitaxial quality. Different dislocation densities can exhibit different CL intensity, either locally or globally [18,19]. The radiative efficiencies of both band-edge (BE) and yellow band (YB) emission in CL spectrum can be directly related to the densities of threading dislocations in the film [19]. Fig. 4 (a) displays the cathodoluminescence (CL) spectra with a 10 kV accelerating voltage at room temperature. The MQWs peak wavelength was 432 nm under two different growth on semipolar GaN film temperature (1100 °C and 1030 °C). As we can see, the CL peak intensity grows 3.7 times higher in 1100 °C sample as compared to the 1030 °C sample. This means better crystalline quality of semipolar GaN film at growth higher temperature [20]. Even though

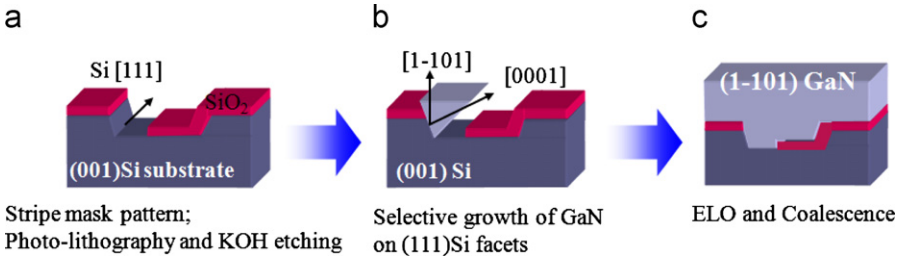

Fig. 1. Schematic fabrication process in the ELO of (1 $\bar{1}$ 0 1) GaN on (0 0 1) Si substrate.

high temperature is preferred to acquire good quality material, we also noticed that the Ga melt etching happened from SEM top view image (Fig. 4(b)). It can be attributed to diffusion of Ga atoms and their interaction with Si atoms leading to Ga meltback etching [21]. This characteristic puts an upper limit for epitaxial growth temperature.

After InGaN/GaN structure was fully grown, several optical tests were performed to analyze the properties of InGaN quantum wells. The PL spectrum as a function of the excitation power for semipolar InGaN/GaN MQWs structure at room temperature is shown in Fig. 5(a). We obtained almost unshifted PL peaks with the increasing excitation power. It means the InGaN/GaN MQWs grown on (1 $\bar{1}$ 0 1) GaN/7 degrees off axis (0 0 1) Si substrate have very low internal piezoelectric field and this leads to the decrease of QCSE [22]. The integrated PL intensity was fitted based on the relation $I \sim P^{\alpha}$ [23], where I is the integrated PL intensity, P is the excitation power density, and α is the power index. The fitting result is shown in Fig. 5(b). The close-to-one power index of our sample ($\alpha = 1.07$) indicates that the radiative recombination dominated the optical transition [24]. From above results, it is suggested that the QCSE is extremely small or absent in our InGaN/GaN MQWs grown on (1$\bar{1}$01) GaN/7 degrees off axis (0 0 1) Si substrate.

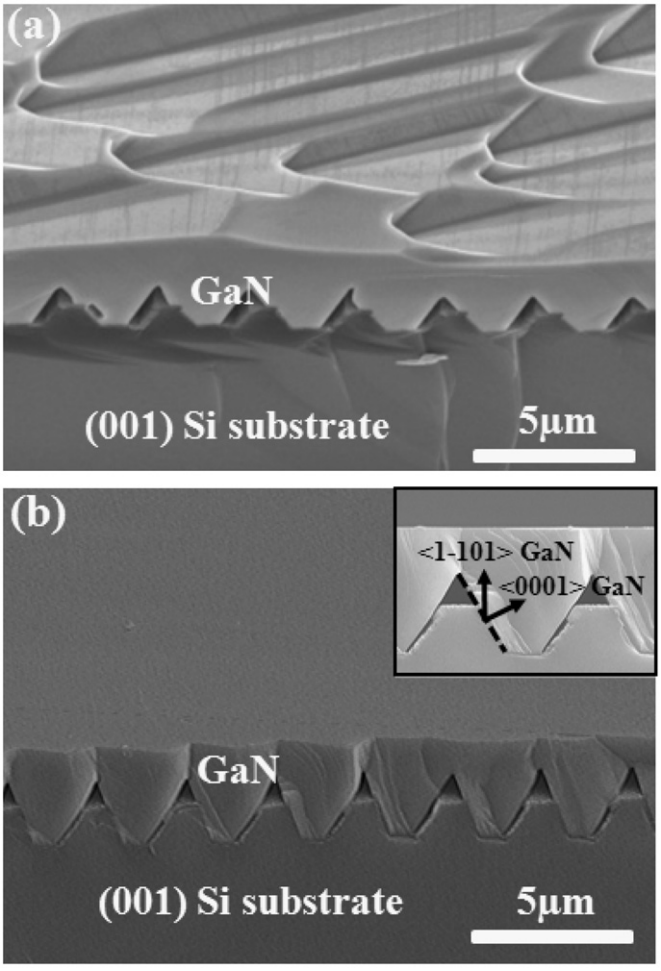

Fig. 2. Cross-section SEM image of the other degrees off axis (0 0 1) Si substrate (a) and the 7 degrees off axis (0 0 1) Si substrate (b). Inset in Fig. 2(b) shows a platelet of (1 $\bar{1}$ 0 1) GaN of the coalesced GaN stripes cross-section SEM image.

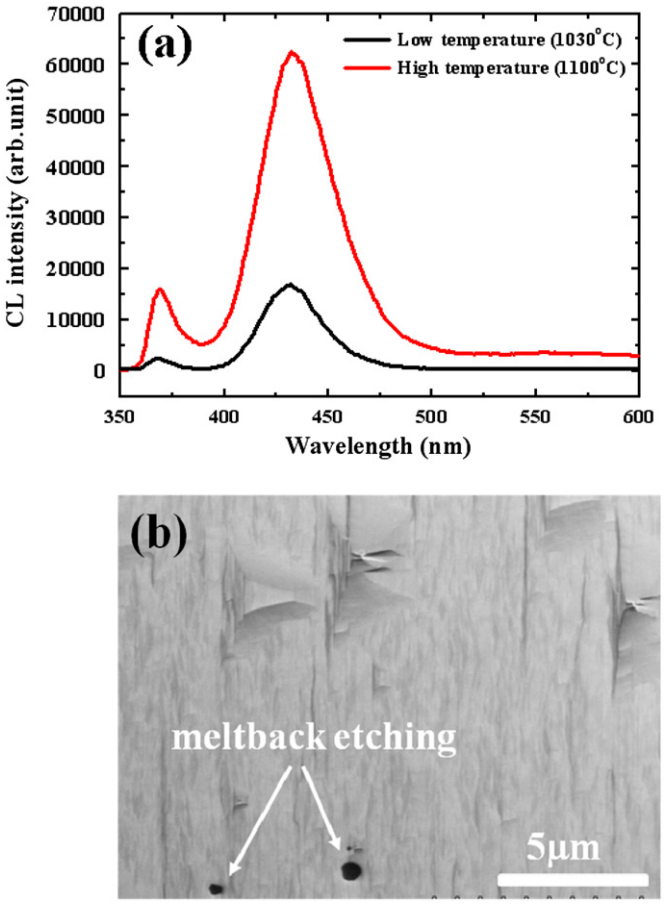

Fig. 4. (a) CL spectra of semipolar InGaN/GaN MQWs at room temperature; (b) top-view SEM image of (1 $\bar{1}$ 0 1) GaN film which deposition temperature is 1100 °C.

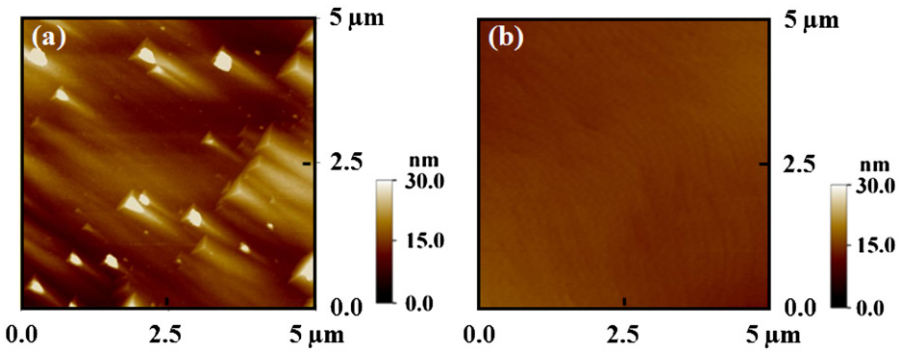

Fig. 3. AFM images of the other degrees off axis (0 0 1) Si substrate (a) and the 7 degrees off axis (0 0 1) Si substrate (b).

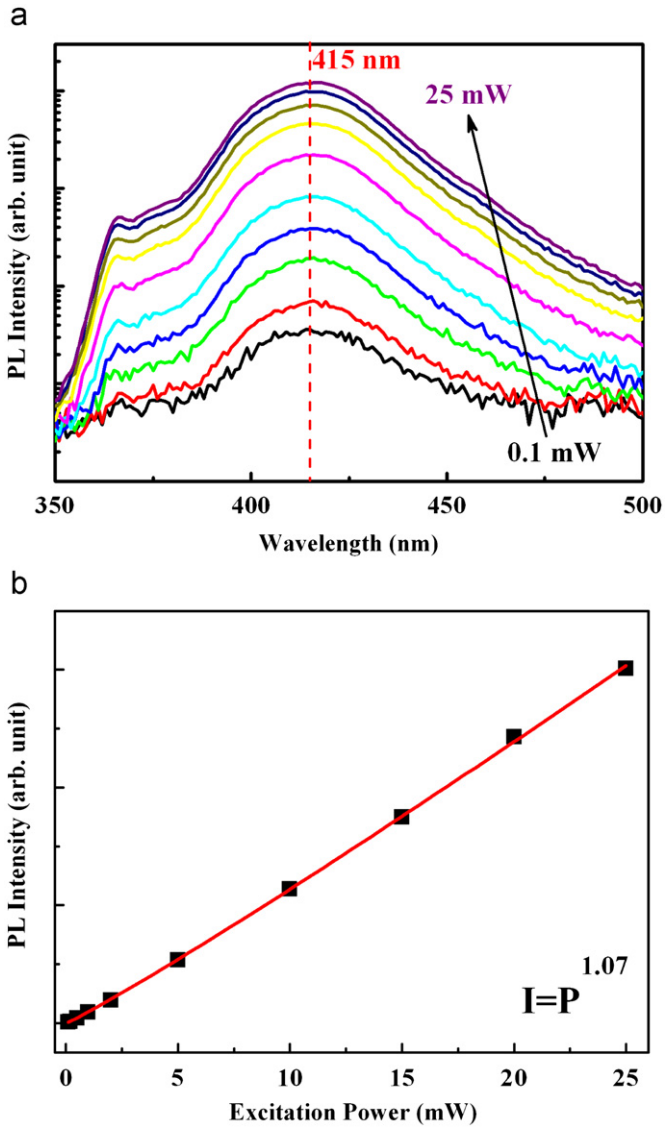

Fig. 5. (a) PL spectra as functions of the excitation power and (b) (Color online) The relation between PL intensity and excitation power density for semipolar InGaN/GaN MQWs at room temperature.

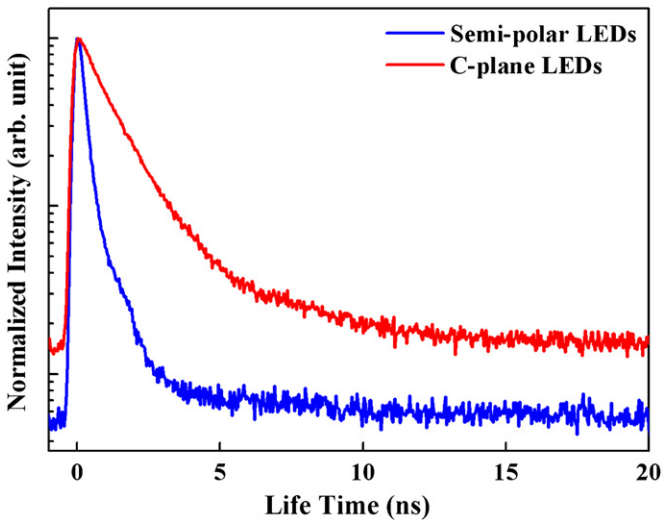

Fig. 6. Low-temperature TRPL of the {1 $\bar{1}$ 0 1} InGaN/GaN MQW and {0 0 0 1} InGaN/GaN MQW.

Time-Resolved PL can be a powerful tool to study carrier recombination dynamics. From previous research, the shorter the lifetime is, the higher the radiative recombination rate will be. The low temperature TRPL decay for both samples was shown in Fig. 6. Because the measurement was carried out at 10 K, the influence of the nonradiative recombination process could be excluded [25]. The TRPL results can be fitted by a biexponential decaying function [26]:

$$I(t) = I_1(0)\exp\left(-\frac{t}{\tau_1}\right) + I_2(0)\exp\left(-\frac{t}{\tau_2}\right) \quad (1)$$

where $I(t)$ is the PL intensity at time t ; τ_1 and τ_2 represent the characteristic lifetimes of the carriers. The fast decay time constant (τ_1) usually represents the radiative recombination of excitons and the relaxation of QW excitons from free or extended states toward localized states [26,27]. Our fitting shows τ_1=0.2 and 1.1 ns for semipolar and c-plane, respectively. The slow decay time (τ_2) accounts for communication between localized states and localized excitons [26,27]. Its fitting shows τ_2=0.7 and 3.8 ns for semipolar and c-plane, respectively. In both fast and slow constants, semipolar's lifetime is generally shorter than c-plane's at low temperature. Typically, the reduction in PL decay time could be attributed to the reduction in internal electric field that leads to increase electron-hole pair recombination probability [28]. This strongly suggests that the highly efficient radiation is more likely in semipolar sample than c-plane sample.

Due to the low crystalline symmetry of the (1 $\bar{1}$ 0 1) plane and the anisotropic compressive strain induced by the lattice mismatch between GaN and InGaN, the PL emitted from semipolar MQWs should exhibit polarization anisotropy [29]. As we expected, the PL intensity varied with angular orientation of the polarizer. The degree of polarization (DOP) is defined as [30]:

$$\rho = \frac{I_{max} - I_{min}}{I_{max} + I_{min}} \quad (2)$$

where I_{max} is the intensity of light with polarization parallel to the Si stripes (corresponding to $<1\,1\,\bar{2}\,0>$ GaN) and I_{min} is the intensity of light with polarization perpendicular to the Si stripes. By utilizing the above-mentioned equation, the DOP was calculated to be 61.2% as shown in Fig. 7 (a). Compared to its c-plane GaN counterpart, which exhibits more isotropic emission (DOP=3.7%) in Fig. 7(b), the difference is quite significant and comply with the previous report [29].

4. Conclusion

In summary, the high quality InGaN/GaN MQWs structure is successfully grown on (1 $\bar{1}$ 0 1) GaN/7 degrees off axis (0 0 1) Si substrate. The smooth coalescence of the stripes and surface morphology was measured by SEM and AFM. The CL spectrum of semipolar InGaN/GaN MQWs shows better crystalline quality of epitaxial layer under higher growth temperature of semipolar GaN film. No obvious emission peak shift is observed from power-dependent PL measurement, which is the evidence of the minimized QCSE. We can further find out semipolar InGaN/GaN MQWs have higher radiative recombination rate due to reduction in internal electric field from TRPL measurement. In addition, it has higher polarization ratio attributed to anisotropic compressive strain due to this semi-polar material.

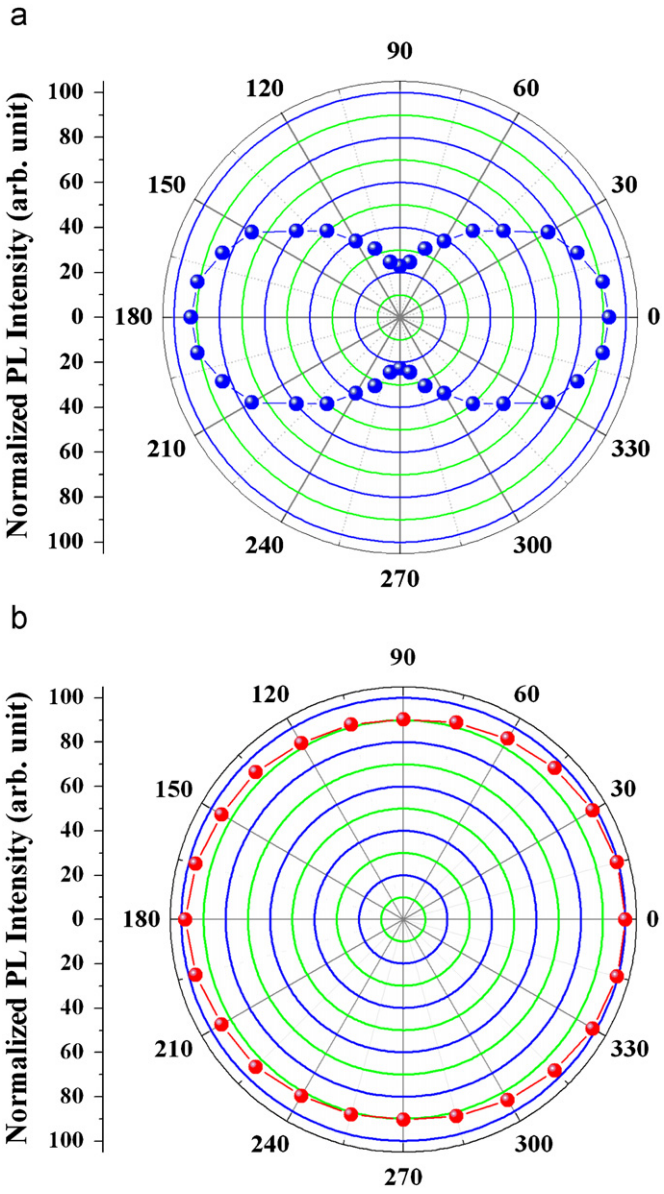

Fig. 7. Variation of PL intensity with angle orientation of the polarizer for growth InGaN/GaN MQWs on (a) semi-polar (b) c-plane Si substrate.

Acknowledgments

The authors are grateful to the National Science Council of the Republic of China, Taiwan, for financially supporting this research under Contract No. NSC 98-2923-E-009-001-MY3.

References

[1] S. Nakamura, M. Senoh, N. Iwasa, T. Yamada, T. Matsushita, H. Kiyoku, Y. Sugimoto, T. Kozaki, H. Umemoto, M. Sano, K. Chocho, Jpn. J. Appl. Phys. 36 (1997) L1586.
[2] S. Keller, R. Vetury, G. Parish, S.P. DenBaars, U.K. Mishra, Appl. Phys. Lett. 78 (2001) 3088.
[3] Y. Narukawa, I. Niki, K. Izuno, M. Yamada, Y. Murazki, T. Mukai, Jpn. J. Appl. Phys. 41 (2002) L371.
[4] T. Takeuhi, H. Amano, I. Akasaki, Jpn. J. Appl. Phys. 39 (Part 1) (2000) 413.
[5] T. Wunderer, P. Brückner, J. Hertkorn, F. Scholz, G.J. Beirne, M. Jetter, P. Michler, M. Feneberg, K. Thonke, Appl. Phys. Lett 90 (2007) 171123.
[6] M. Ueda, K. Kojima, M. Funato, Y. Kawakami, Y. Narukawa, T. Mukai, Appl. Phys. Lett 89 (2006) 211907.
[7] T. Takeuhi, H. Amano, I. Akasaki, Jpn. J. Appl. Phys. 39 (Part 1) (2000) 413.
[8] S.H. Park, J. Appl. Phys. 91 (2002) 9904.
[9] Baoshun Zhang, Hu Liang, Yong Wang, Zhihong Feng, Kar Wei Ng, Kei May Lau, J. Crystal Growth 298 (2007) 725.
[10] A. Krost, A. Dadgar, Materials Science and Engineering B 93 (2002) 77.
[11] Z. Mao, S. McKernan, C.B. Carter, W. Yang, S.A. McPherson, MRS Internet J. Nitride Semicond. Res. 4S1 (1999) G3.13.
[12] H. Marchand, N. Zhang, L. Zhao, Y. Golan, S.J. Rosner, G. Girolami, P.T. Fini, J.P. Ibbetson, S. Keller, S. DenBaars, J.S. Speck, U.K. Mishra, MRS Internet J. Nitride Semicond. Res. 4 (1999) 2.
[13] N.P. Kobayashi, J.T. Kobayashi, X. Zhang, P.D. Dapkus, D.H. Rich, Appl. Phys. Lett. 74 (1999) 2836.
[14] Shigeyasu Tanaka, Yasutoshi Kawaguchi, Nobuhiko Sawaki, Michio Hibino, Kazumasa Hiramatsu, Appl. Phys. Lett. 76 (2000) 2701.
[15] Y. Honda, N. Kameshiro, M. Yamaguchi, N. Sawaki, J. Crystal Growth 242 (2002) 82.
[16] Nobuhiko Sawaki, Toshiki Hikosaka, Norikatsu Koide, Shigeyasu Tanaka, Yoshio Honda, Masahito Yamaguchi, J. Crystal Growth 311 (2009) 2867.
[17] Harald Brune, Marcella Giovannini, Karsten Bromann, Klaus Kern, Nature 394 (1998) 451–453.
[18] Naoyuki Ino, Naoki Yamamoto, Appl. Phys. Lett. 93 (2008) 232103.
[19] N. Yamamoto, H. Itoh, V. Grillo, S.F. Chichibu, S. Keller, J.S. Speck, S.P. DenBaars, U.K. Mishra, S. Nakamura, G. Salviati, J. Appl. Phys. 94 (2003) 4315.
[20] J.T. Kobayashi, N.P. Kobayashi, X. Zhang, P.D. Dapkus, D.H. Rich, Structural and optical emission characteristics of InGaN thin layers and the implications for growing high-quality quantum wells by MOCVD, Journal of Crystal Growth 195 (1998) 252–257.
[21] Hiroyasu Ishikawa, Kensaku Yamamoto, Takashi Egawa, Tetsuo Soga, Takashi Jimbo, Masayoshi Umeno, J. Crystal Growth 189 (1998) 178.
[22] Hongbo Yu, L.K. Lee, Taeil Jung, P.C. Ku, Appl. Phys. Lett. 90 (2007) 141906.
[23] C.H. Chiu, S.Y. Kuo, M.H. Lo, C.C. Ke, T.C. Wang, Y.T. Lee,1, H.C. Kuo, T.C. Lu, S.C. Wang, J. Appl. Phys. 105 (2009) 063105.
[24] E. Kuokstis, C.Q. Chen, M.E. Gaevski, W.H. Sun, J.W. Yang, G. Simin, M.A. Khan, Appl. Phys. Lett. 81 (2002) 4130.
[25] T. Onuma, A. Chakraborty, B.A. Haskell, S. Keller, S.P. DenBaars, J.S. Speck, S. Nakamura, U.K. Mishra, Appl. Phys. Lett. 86 (2005) 151918.
[26] W.Z. Lee, G.W. Shu, J.S. Wang, J.L. Shen, C.A. Lin, W.H. Chang, R.C. Ruaan, W.C. Chou, C.H. Lu, Y.C. Lee, Nanotechnology 16 (2005) 1517–1521.
[27] T.S. Ko, T.C. Lu, T.C. Wang, J.R. Chen, R.C. Gao, M.H. Lo, H.C. Kuo, S.C. Wang, J.L. Shen, J. Appl. Phys. 104 (2008) 093106.
[28] P. Waltereit, O. Brandt, A. Trampert, H.T. Grahn, J. Menniger, M. Ramsteiner, M. Reiche, K.H. Ploog, Nature 406 (2000) 865.
[29] M. Ueda, K. Kojima, M. Funato, Y. Kawakami, Y. Narukawa, T. Mukai, Appl. Phys. Lett. 89 (2006) 211907.
[30] Yue Jun Sun, Oliver Brandt, Manfred Ramsteiner, Holger T. Grahn, Klaus H. Ploog, Appl. Phys. Lett. 82 (2003) 3850.